Land–Ocean Shifts in Tropical Precipitation Linked to Surface Temperature and Humidity Change

F. HUGO LAMBERT AND ANGUS J. FERRARO

College of Engineering, Mathematics and Physical Sciences, University of Exeter, Exeter, United Kingdom

ROBIN CHADWICK

Met Office Hadley Centre, Exeter, United Kingdom

(Manuscript received 30 August 2016, in final form 27 January 2017)

ABSTRACT

A compositing scheme that predicts changes in tropical precipitation under climate change from changes in near-surface relative humidity (RH) and temperature is presented. As shown by earlier work, regions of high tropical precipitation in general circulation models (GCMs) are associated with high near-surface RH and temperature. Under climate change, it is found that high precipitation continues to be associated with the highest surface RH and temperatures in most CMIP5 GCMs, meaning that it is the ''rank'' of a given GCM grid box with respect to others that determines how much precipitation falls rather than the absolute value of surface temperature or RH change, consistent with the weak temperature gradient approximation. Further, it is demonstrated that the majority of CMIP5 GCMs are close to a threshold near which reductions in land RH produce large reductions in the RH ranking of some land regions, causing reductions in precipitation over land, particularly South America, and compensating increases over ocean. Recent work on predicting future changes in specific humidity allows the prediction of the qualitative sense of precipitation change in some GCMs when land surface humidity changes are unknown. However, the magnitudes of predicted changes are too small. Further study, perhaps into the role of radiative and land–atmosphere feedbacks, is necessary.

1. Introduction

Changes in regional precipitation in the tropics per Kelvin warming under a given climate change scenario differ substantially across contemporary general circulation models (GCMs) (Collins et al. 2013). In an effort to understand the differences, researchers have employed a number of schemes or ''decompositions'' that express precipitation changes in terms of a number of physically interpretable components (e.g., Emori and Brown 2005; Bony et al. 2013; Chadwick et al. 2013, 2014; Wills et al. 2016). Decompositions have been derived in a variety of ways, but most have components identified as ''thermodynamic,'' which are due to changes in atmospheric moisture, and ''dynamic,'' which are due to changes in the intensity and location of atmospheric circulation features. The terms can be subdivided. Relevant to our study, the dynamic term may be split into a ''weakening'' term that describes precipitation changes due to the slowing down of atmospheric circulation under global warming, and a ''shift'' term that describes movement of precipitation patterns.

The thermodynamic term can be estimated by combining changes in surface specific humidity (SH), which dominate changes in atmospheric moisture under climate change, with the climatological (i.e., unperturbed) atmospheric circulation to predict changes in moisture convergence and therefore changes in precipitation that would occur if other factors were unaltered. Over tropical oceans, a typical GCM maintains near-constant relative humidity (RH) under climate change. Hence fractional changes in near-surface SH follow fractional changes in saturation SH predicted by the Clausius–Clapeyron equation.

Supplemental information related to this paper is available at the Journals Online website: http://dx.doi.org/10.1175/JCLI-D-16-0649.s1.

Corresponding author: F. Hugo Lambert, f.h.lambert@exeter.ac.uk

DOI: 10.1175/JCLI-D-16-0649.1

The thermodynamic change in precipitation over oceans is therefore an increase of about 7% K^{-1}. Increases over land can be smaller if there are reductions in land RH. The weakening term can be estimated by combining changes in atmospheric circulation with the climatological moisture field. GCMs predict a slowing down of the tropical circulation and an associated reduction in precipitation of about 3% or 4% K^{-1}, which reflects the fact that the demand for convective heating of the atmosphere increases at a lower rate than the availability of moisture at the surface (e.g., Vecchi and Soden 2007). The combined effect of the thermodynamic and weakening terms is an increase in precipitation of about 3% K^{-1} in regions of climatological atmospheric convergence and a small reduction or no change in regions of divergence (the latter typically experience little climatological precipitation) that is known as the ''rich-get-richer'' response (Mitchell et al. 1987; Chou and Neelin 2004; Held and Soden 2006). The residual difference between GCM-simulated precipitation change and the sum of the so-called thermodynamic and weakening terms can then be attributed to what we call shifts, which represent the movement of precipitation patterns. A problem is that these shifts are poorly understood but typically large. In particular, they dominate the meridional mean zonally asymmetric response (Chadwick et al. 2013; Wills et al. 2016), governing the key impact-relevant question of whether areas of precipitation will shift onto or away from land in future (Allan 2014; Hawkins et al. 2014; Good et al. 2016).

Prompted by the need to understand changes in the land–sea contrast of tropical precipitation, in this paper we develop and test a new compositing scheme that estimates shifts in precipitation from patterns of surface temperature and humidity change without the need to rely on residuals. We concentrate on meridional mean change because a substantial literature on zonal mean change and its relationship to aerosol forcing and interhemispheric energy budget imbalance already exists (e.g., Yoshimori and Broccoli 2008; Scheff and Frierson 2012; Chiang et al. 2013; Hwang et al. 2013) and because GCM-simulated response is more obviously connected with asymmetries in surface properties caused by zonal variations in land fraction than in the zonal mean case. (We do make zonal mean results and maps available in the online supplemental information for reference.) The remainder of the paper is arranged as follows: in section 2, we explain the scheme and how it is motivated by earlier theory. In section 3, we describe the GCM data that we will use to test the scheme. Section 4 contains the results, showing the extent to which GCMs conform to the scheme. The scheme is a classification to aid understanding and not a prognostic theory of future precipitation change. In section 5, however, we show what can be achieved without knowledge of land humidity change as a first step toward a prognostic theory. Section 6 presents a discussion of the implications of our results and section 7 is a short summary of our main conclusions.

2. Precipitation compositing scheme

a. Theoretical and modeling background

The unique conditions that exist near the equator allow a simple interpretation of many features of tropical climate (Schneider 1977). Specifically, the weakness of the Coriolis force prevents the tropical free atmosphere above about 700 hPa from maintaining large horizontal gradients of pressure or temperature. This is termed the ''weak temperature gradient'' approximation. Horizontal variations in moisture content in the free troposphere do exist, but these are dwarfed by variations at the surface. The result is that the occurrence of clouds and precipitation in the tropics can be anticipated through some measure of the relationship between conditions in the local atmospheric boundary layer, which may vary substantially, and mean conditions in the free atmosphere. Although organized systems such as tropical waves and cyclones do occur, a large volume of work has developed understanding of precipitation and cloud by treating the tropics as a set of vertical columns that interact only via the ''mean field'' of the nearly uniform free atmosphere (Sobel and Bretherton 2000). Many studies have achieved this through composites, which group different geographical locations by similar local properties, to classify local behavior into sets of regimes with common features allowing easier interpretation. Bretherton et al. (2004) and Biasutti et al. (2006) grouped climatological precipitation by precipitable water and near-surface RH; Emori and Brown (2005) grouped changes in precipitation by 500-hPa vertical velocity; Allan (2012) grouped changes in precipitation by 500-hPa vertical velocity and surface temperature; Wyant et al. (2009) grouped changes in low cloud relevant to radiative feedbacks using lower-tropospheric stability, which is the difference between near-surface and 700-hPa potential temperature; Lambert and Taylor (2014) and Ferraro et al. (2015) grouped clear-sky radiative feedbacks by near-surface temperature and precipitation; and Webb et al. (2015) grouped cloud radiative feedbacks by precipitation in convecting regions. The last three articles demonstrate that the robustness of these mean-field ideas is such that even precipitation itself is a useful compositing variable under tropical conditions.

These and other studies reveal that convection and precipitating cloud regimes are associated with high precipitable water, upward vertical velocity, high

surface temperature, and low lower-tropospheric stability, and that nonprecipitating low cloud regimes are associated with low precipitable water, downward vertical velocity, low surface temperature, and high lower-tropospheric stability. For surface temperature and precipitable water in particular, it is important to recognize that it is for the most part not the absolute values of these quantities that determine climatic regime, but the local value of the quantity relative to the tropical mean. Meanwhile, total precipitation amount in the tropics is largely controlled by the requirement that atmospheric radiative cooling and energetic export to the extratropics balance convective heating. Increases in surface temperature do not therefore result in substantial increases in the area of the tropical convecting region (Pierrehumbert 1995; Johnson and Xie 2010). Where surface temperature increases are spatially heterogeneous, however, the location of precipitation may change. Xie et al. (2010) showed that patterns of precipitation change over ocean are associated with patterns of sea surface temperature change.

Theoretical and numerical modeling studies have taken advantage of the above constraints to predict tropical precipitation and cloud amounts. Neelin and Held (1987) used the weak temperature gradient approximation along with the vertically integrated moist static energy budget to derive horizontal atmospheric convergence in the tropics, and therefore vertical velocity and precipitation. Sobel and Bretherton (2000) showed that a set of single vertical column models coupled only via a mean free tropospheric temperature can represent the results of a full atmospheric model reasonably well. Blossey et al. (2009) and Dal Gesso et al. (2015) among other studies have found that single-column models have some use in predicting GCM cloud amounts in stable subsiding regimes. Using the ideas introduced here, in the next subsection we describe our compositing scheme for predicting precipitation changes from the relationship between local conditions and the tropical mean.

b. *Compositing scheme description*

We take monthly-mean gridbox precipitation data for 30°N–30°S from the unforced preindustrial control run of a GCM (the data are described in section 3) and regrid so that all runs are on a 2.5° longitude by 2.5° latitude grid. A composite is then formed by grouping grid boxes into 10 equal-population bins of ascending near-surface RH. Every grid box is therefore assigned to a RH bin based on its ''rank'' relative to other grid boxes rather than its absolute value of RH. Each RH bin is then further divided into 10 equal-population bins of ascending near-surface temperature, T_S. The resulting RH–T_S bins are assigned a precipitation value that is equal to the area-weighted average of the gridbox precipitation in that bin. We divide into bins of RH first because we find a broader range of T_S in each RH bin than we find RH in T_S bins if the composite is formed in reverse order. We choose RH and T_S as compositing variables because their variation across the tropics is strongly linked to variations in moist static energy and lower-tropospheric stability, and because they are observable quantities in principle. Further, variations in T_S have been shown to be strongly related to precipitation amounts across tropical oceans (e.g., Bretherton et al. 2004; Biasutti et al. 2006; Xie et al. 2010); variations in RH are quite small over the ocean, but can be a crucial control on the initiation of convective precipitation over land (e.g., Eltahir 1998; Betts 2004; Fasullo 2012; Chadwick 2016). Our expectation is that the highest RH and T_S bins will experience heavy precipitation, while low RH and T_S bins will experience little precipitation.

We predict shifts in monthly-mean precipitation in a $4\times CO_2$ simulation of a GCM by associating them with the RH and T_S for that month. We reclassify each 30°N–30°S grid box into a new ''perturbed'' bin based on the rank of its new $4\times CO_2$ RH and T_S values. Grid boxes move to higher bins where their new RH and T_S values rank higher than their control values and move to lower bins where the RH and T_S values rank lower. The predicted precipitation shift is the difference between the control precipitation value associated with the perturbed bin and the control precipitation value associated with the control bin. We therefore assume that the preferred bins for both heavy precipitation and low precipitation in a perturbed run will continue to be those with the same rankings of RH and T_S as in the control. Precipitation in a given RH–T_S regime remains unchanged because we continue to use the control precipitation associated with each composite bin. Finally, we calculate annual mean results by taking the mean over the monthly predictions for each model. This process defines our shift component.

Thermodynamic and weakening changes in precipitation are predicted through a simplification of the scaling argument used by Chadwick et al. (2013). We scale the precipitation amounts of each composite bin by the tropical mean change in precipitation per Kelvin warming. This is equivalent to assuming that surface SH (thermodynamic) and tropospheric circulation (weakening) in every grid box change in proportion to tropical mean changes in these variables, consistent with GCM studies of the rich-get-richer mechanism (Held and Soden 2006; Vecchi and Soden 2007; Ma et al. 2012). Our null hypothesis is that in the ''bin space'' of the precipitation composite, precipitating features do not change location (see also Allan 2012). We test this

assertion by comparing this scaled composite with the perturbed composite formed when $4\times CO_2$ precipitation amounts are composited on $4\times CO_2$ T_S and RH values. There is no need to investigate thermodynamic and weakening changes geographically. Finally, we gauge the overall success of our scheme by making a geographical comparison of GCM $4\times CO_2$ precipitation change with respect to control with the change predicted by using the scaled composite and $4\times CO_2$ T_S and RH values. As a consistency check, the geographical precipitation change when the perturbed composite is used to estimate perturbed precipitation amounts is calculated. This is the maximum fidelity that can be achieved with our method, because control and perturbed RH and T_S, and control precipitation values, are known accurately. Mathematically, our composite predictions can be written as

$$\Delta P_{\text{shift}} = P_{\text{con}}(\text{RH}_{\text{pert}}, T_{S,\text{pert}}) - P_{\text{con}}(\text{RH}_{\text{con}}, T_{S,\text{con}}),$$
$$\Delta P_{\text{scaled}} = P_{\text{scaled}}(\text{RH}_{\text{pert}}, T_{S,\text{pert}}) - P_{\text{con}}(\text{RH}_{\text{con}}, T_{S,\text{con}}),$$
$$\Delta P_{\text{pert}} = P_{\text{pert}}(\text{RH}_{\text{pert}}, T_{S,\text{pert}}) - P_{\text{con}}(\text{RH}_{\text{con}}, T_{S,\text{con}}),$$

where ΔP_{shift} are predicted changes in precipitation due to shifts, ΔP_{scaled} are predicted changes in precipitation due to shifts and thermodynamic and dynamic effects, and ΔP_{pert} are predicted changes in precipitation where all GCM perturbed and control values are known, serving to show the best that can be achieved with the compositing method. The P are precipitation composite values for a given RH and T_S. RH and T_S values subscripted with ''con'' are control values and values subscripted with ''pert'' are perturbed values.

To explain our expectations and assist understanding of possible precipitation shifts, consider the following example. Under climate change, land regions tend to warm more than ocean regions (e.g., Sutton et al. 2007; Zhang and Li 2016a,b). An ocean region that warms 4 K under a $4\times CO_2$ forcing may find itself in a lower T_S bin than in the control climate because tropical land regions may warm 5 or 6 K. We might therefore anticipate shifts in precipitation and accompanying atmospheric convection from ocean to land because the ocean will be less warm with respect to the tropical mean than it was in the control climate. However, land regions may also experience reductions in RH under warming (e.g., Rowell and Jones 2006). Given that oceanic regions tend to retain approximately constant RH under climate change, land regions with decreasing RH may therefore find themselves moving to lower RH bins. This could produce a shift in precipitation and convection away from these land regions to other, especially oceanic, regions where RH changes little. We expect that the competition between relatively larger warming over land increasing precipitation and relatively larger decreases in RH over land decreasing precipitation will determine whether precipitation patterns shift toward or away from land.

The method makes simplifications that limit or omit the representation of some physical processes. The effects of clear-sky and cloudy-sky radiative feedbacks that may drive changes in precipitation are implied as being associated with meteorological variables that shift following our compositing scheme rather than being considered directly. The same is true of shifts in atmospheric circulation, which we assume to be coincident with shifts in precipitation. This neglects the influence of changes in geographical temperature gradients, which may drive or be driven by changes in dynamics with consequences for precipitation. One example is the weakening of the zonal equatorial Pacific temperature gradient found in many GCMs under warming that leads to a weakening in the Pacific Walker (i.e., zonal) circulation (Zhang and Li 2016b). The location of precipitation may also be affected by atmospheric dynamics not simply related to surface temperature gradients. It has been proposed that monsoon rainfall is controlled by the interaction between tropical dynamics and extratropical planetary waves, which may or may not depend on land–sea temperature gradients (Bordoni and Schneider 2008; Shaw 2014).

The effects of fast adjustments on precipitation, which occur as a result of radiative forcing and which are essentially independent of large-scale sea surface temperature (SST) change, are considered only through their effects on land surface warming. In the tropics, fast adjustments to CO_2 forcing are expected to produce reductions in precipitation over ocean and increases over land associated with heat transport from land to ocean that attempts to maintain a near-time-invariant ratio of land to ocean surface temperature change (Lambert et al. 2011; Bony et al. 2013). These effects are significant in GCMs, linked to land surface warming and therefore at least partially represented by our method, but are small compared with SST-driven changes (Chadwick et al. 2014). It is found that the effects of fast adjustment and sea surface temperature on precipitation add quite linearly when trialed separately and simultaneously in a GCM (Lambert et al. 2011; Chadwick et al. 2014). We therefore do not expect issues for precipitation simulation related to the GCM simulations we use not being in equilibrium (see section 3). Further effects occur, however, when radiative forcings cause changes in atmospheric heating without first affecting the surface (e.g., Previdi 2010; Andrews et al. 2012). For the uniform CO_2 forcing considered in our

TABLE 1. CMIP5 GCMs used in this study. ''Atmospheric grid'' refers to the number of points in longitude and latitude. If the model is spectral the resolution given is the resolution of its geometric transform grid; the spectral resolution is given in brackets. (Expansions of acronyms are available online at http://www.ametsoc.org/PubsAcronymList.)

Model	Institute ID	Atmospheric grid	Reference
ACCESS1.0	CSRIO-BOM	192 × 144	Bi et al. (2013)
ACCESS1.3	CSRIO-BOM	192 × 144	Bi et al. (2013)
BCC-CSM1.1	BCC	128 × 64 (T42)	Wu et al. (2014)
BCC-CSM1.1-M	BCC	320 × 160 (T106)	Wu et al. (2014)
BNU-ESM	GCESS	128 × 64 (T42)	Ji et al. (2014)
CCSM4	NCAR	288 × 192	Gent et al. (2011)
CNRM-CM5	CNRM-CERFACS	256 × 128 (T127)	Voldoire et al. (2013)
CanESM2	CCCMA	128 × 64 (T63)	von Salzen et al. (2013)
FGOALS-s2	LASG-IAP	128 × 104 (R42)	Bao et al. (2013)
GFDL-CM3	NOAA GFDL	144 × 90	Donner et al. (2011)
GFDL-ESM2G	NOAA GFDL	144 × 90	Dunne et al. (2012)
GFDL-ESM2M	NOAA GFDL	144 × 90	Dunne et al. (2012)
GISS-E2-H	NASA GISS	144 × 90	Schmidt et al. (2014)
GISS-E2-R	NASA GISS	144 × 90	Schmidt et al. (2014)
HadGEM2-ES	MOHC	192 × 144	Martin et al. (2011)
INMCM4	INM	180 × 120	Volodin et al. (2010)
IPSL-CM5A-LR	IPSL	96 × 96	Dufresne et al. (2013)
IPSL-CM5A-MR	IPSL	143 × 144	Dufresne et al. (2013)
IPSL-CM5B-LR	IPSL	96 × 96	Dufresne et al. (2013)
MIROC-ESM	MIROC	128 × 64 (T42)	Watanabe et al. (2011)
MIROC5	MIROC	256 × 128 (T85)	Watanabe et al. (2010)
MRI-CGCM3	MRI	320 × 160 (T159)	Yukimoto et al. (2012)
NorESM1-M	NCC	144 × 96	Bentsen et al. (2013)

study, regional variations in atmospheric heating are small relative to the size of mean heating. Shifts in precipitation may not therefore be greatly affected. We note, though, that the highly nonuniform (both vertically and horizontally) atmospheric heating applied by black carbon aerosol during historical and future climate change scenario forcing may pose a problem for our method (Ming et al. 2010; Previdi 2010; Frieler et al. 2011). Predicting changes in precipitation in more realistic twenty-first-century scenarios may therefore be more difficult. Land–atmosphere feedbacks are not considered explicitly. Some of these drive changes in T_S and RH, but others may have more subtle influence through changes in surface fluxes or boundary layer conditions (e.g., Eltahir 1998) or cloud condensation nuclei concentration (e.g., Krejci et al. 2005).

Our scheme is not a prognostic theory, because it relies on knowledge of perturbed RH and T_S and it is unclear to what extent changes in precipitation drive or are driven by changes in RH and T_S. (The possibility of developing a prognostic scheme is discussed in section 5.) Despite these limitations, it is useful because it allows us to explore the extent to which changes in tropical RH, T_S, and precipitation represent a coupled problem in GCMs and, where successful, it gives us a physical basis for understanding the shift component of precipitation change. It is shown in section 4 that differences in GCM control states exert a strong control on differences in precipitation shifts in the perturbed simulations. This has implications for what the observed mean state and variability may tell us about real future tropical precipitation change, as discussed in section 6.

3. GCM data

We analyze GCM simulations from phase 5 of the Coupled Model Intercomparison Project (CMIP5) (Taylor et al. 2012). The models used, their horizontal resolutions, and accompanying references are shown in Table 1. We take data from the model preindustrial control simulations (piControl, hereinafter referred to as ''control''), in which atmospheric CO_2 concentration is held fixed at 287 ppmv, and their abrupt carbon dioxide quadrupling simulations (abrupt4×CO2, hereinafter referred to as $4\times CO_2$), in which CO_2 concentration is instantaneously quadrupled to 1148 ppmv at the beginning of the run. One ensemble member is used in each case. All GCMs are fully coupled, featuring coupled interactive atmospheres, oceans, sea ice, and land surfaces. Only the atmospheric carbon cycle is constrained to prescribed values. Our analysis uses monthly means of the last 30 years from every simulation. In the case of the 150-yr-long $4\times CO_2$ simulations this means that most forced global warming has occurred, but that the simulations are not at

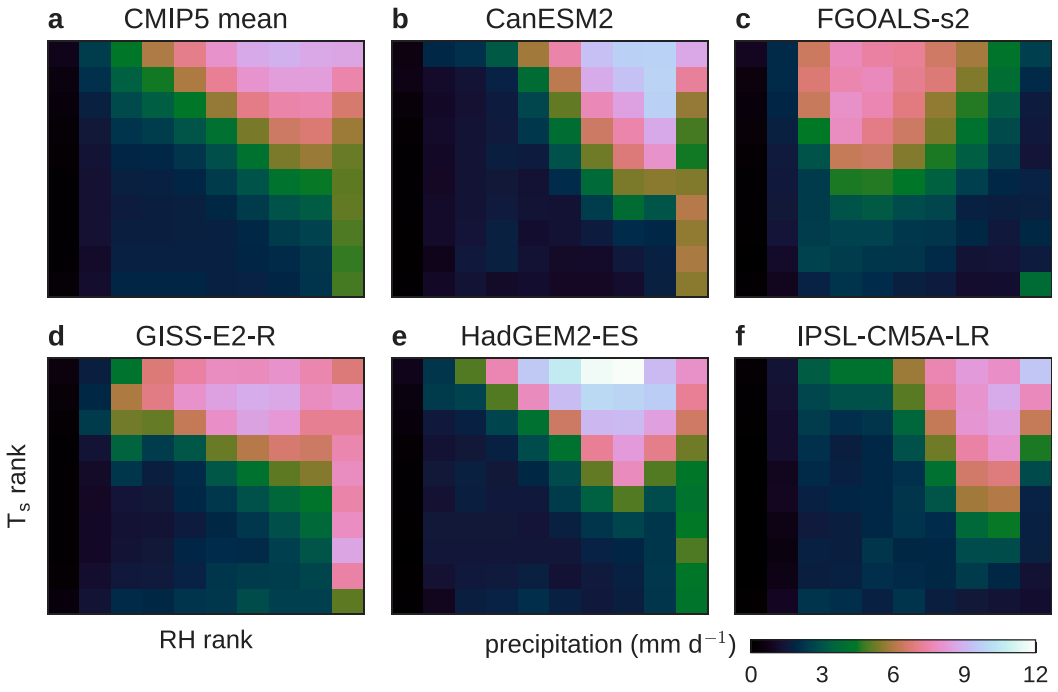

FIG. 1. Composites of control tropical precipitation on control RH and T_S for (a) the CMIP5 model mean and our five marker models: (b) CanESM2, (c) FGOALS-s2, (d) GISS-E2-R, (e) HadGEM2-ES, and (f) IPSL-CM5A-LR. In general, the heaviest precipitation falls in the highest RH and T_S bins. FGOALS-s2 is an exception, heavy precipitation tending to fall in lower T_S bins than in the CMIP5 mean.

equilibrium. [Caldeira and Myhrvold (2013) estimated that 4×CO_2 simulations realize about 70% of their equilibrium warming after 100 years.]

4. RH–T_S composite results

We now present our RH–T_S composites. To focus the discussion, we show results largely for the CMIP5 mean and five marker models: CanESM2, FGOALS-s2, GISS-E2-R, HadGEM2-ES, and IPSL-CM5A-LR, which are chosen to highlight qualitatively different responses within the ensemble and because our compositing scheme has different levels of success in predicting GCM-simulated changes. Because we are primarily interested in the zonally asymmetric response and land–ocean shifts in precipitation in particular, we show results for the meridional mean alone in the main manuscript. The 4×CO_2–control results are shown per Kelvin tropical mean (30°N–30°S) warming to aid intermodel comparability, apart from where explicitly stated. Further results for all models, including zonal mean responses and maps and maps of RH and T_S rank locations and changes, are given in the online supplemental material.

RH–T_S control composites of control precipitation on control RH and T_S are shown in Fig. 1 for the CMIP5 mean and our marker models. In general, the heaviest precipitation falls in the highest RH and T_S bins as expected, although FGOALS-s2 is an exception, with heavy precipitation tending to fall in lower RH bins than in the CMIP5 mean. The mean RH and T_S values of each bin are shown as blue points in Fig. 2 for the CMIP5 mean and the five marker models. RH bins tend to be separated by very small differences in RH of around 1%, apart from the highest and especially the two lowest bins. Bins are more evenly spaced in T_S, with some crowding at the upper end. The proportion of land found in each control composite bin is shown in the left-hand side of each panel of Fig. 3. In the majority of models, land is most common in the highest and especially the lowest RH bins. FGOALS-s2 and IPSL-CM5A-LR are exceptions, where land is mostly present in the lowest RH bins only. Models with large amounts of land in high RH bins (e.g., CanESM2, GISS-E2-R, and HadGEM2-ES) have the potential for large shifts in precipitation away from land because small RH reductions could cause large reductions in the RH rank of land grid boxes.

a. *Changes in the RH–T_S composites under climate change*

Figure 4 shows 4×CO_2 minus control changes in the composite bins for the CMIP5 mean and our marker GCMs (left-hand side of each panel) and changes

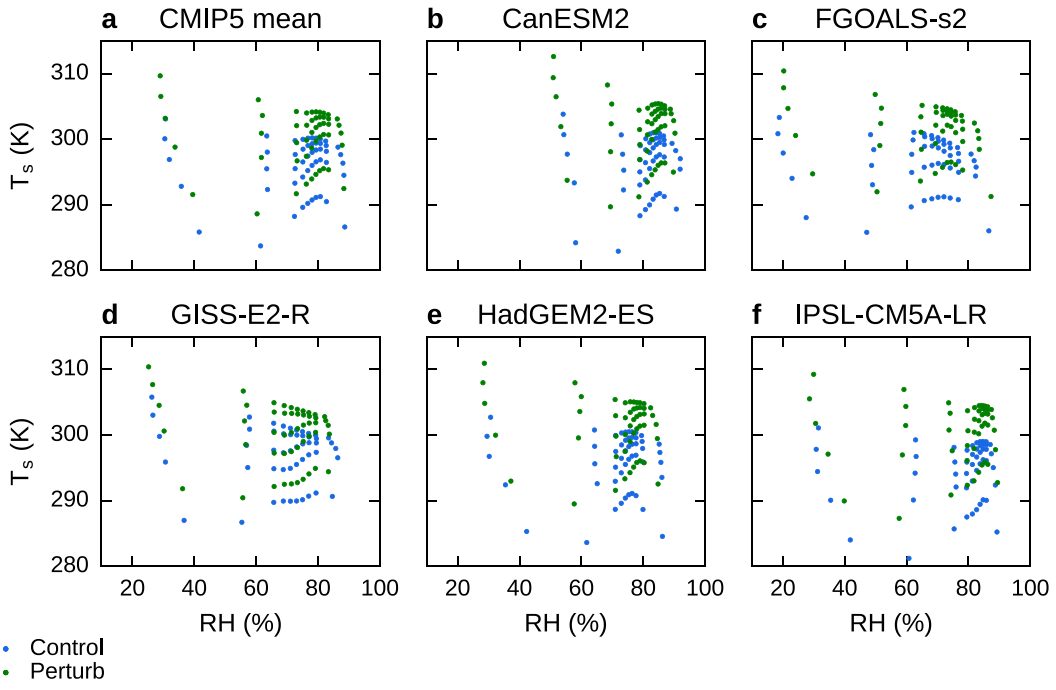

FIG. 2. Mean RH and T_S values for each precipitation RH–T_S bin for the control composites (blue) and the perturbed composites (green) in (a) the CMIP5 mean and (b)–(f) our five marker models.

anticipated from mean precipitation scaling of each control bin (right-hand side of each panel). (See section 2b for an explanation of scaling, which is designed to emulate thermodynamic and weakening changes in the perturbed climate.) The scaling prediction is not successful in reproducing GCM-simulated changes in individual models, which contain a great deal of structure that the scaling does not reproduce. In particular, the GCM-simulated changes predict substantial reductions in precipitation in some bins, which cannot be anticipated via uniform scaling. The prediction for the CMIP5 mean is better, but similarly represents the simulated structure poorly. These issues are underlined by Fig. 5, which shows summary statistics relating GCM-simulated to predicted changes for all GCMs. (Numbers are shown in Table S1 of the supplemental information.) Correlations for other GCMs are higher than in our marker models in a number of cases, but the ordinary least squares (OLS) slope found when scaled predictions are regressed on simulated changes is substantially less than 1 in all cases, indicating that simulated variance is not represented by the scaling. Clearly, it is not the case that precipitation features remain static in the composite bin space with changes described by a simple uniform percentage rich-get-richer increase everywhere.

Perturbed values of mean RH and T_S for each composite bin are shown as green points in Fig. 2. As expected under global warming, all bins move to higher values of T_S. There are also some small increases and decreases in RH. Changes in RH values or changes in the spacing of T_S values can cause changes in precipitation that are not anticipated by our simple scaling prediction. Another issue is the large migration of land grid boxes from high to low RH bins in the perturbed climate (see Fig. 3, right-hand side of panels). Given the differences in physical processes controlling convection over land and ocean, land and ocean grid boxes of a given RH–T_S rank may show rather different precipitation amounts, introducing unpredictable changes into the perturbed composites under climate change. This is a weakness of our compositing scheme, discussed further in section 6. Thus, our ability to predict changes in precipitation composite bins is limited. Despite this, in the next subsection we find that our framework is able to make useful predictions of geographical precipitation change.

b. *Changes in meridional mean precipitation*

Figure 6 presents $4\times CO_2$ minus control perturbations in 30°N–30°S meridional mean precipitation for the CMIP5 mean and our marker models. GCM-simulated values mostly show increases in precipitation over the Pacific, decreases in precipitation over South America, and mixed responses over the Maritime Continent and Africa. Control composite predictions, ΔP_{shift}, which are the difference between the control precipitation value in the perturbed RH–T_S bin and the control RH–T_S bin,

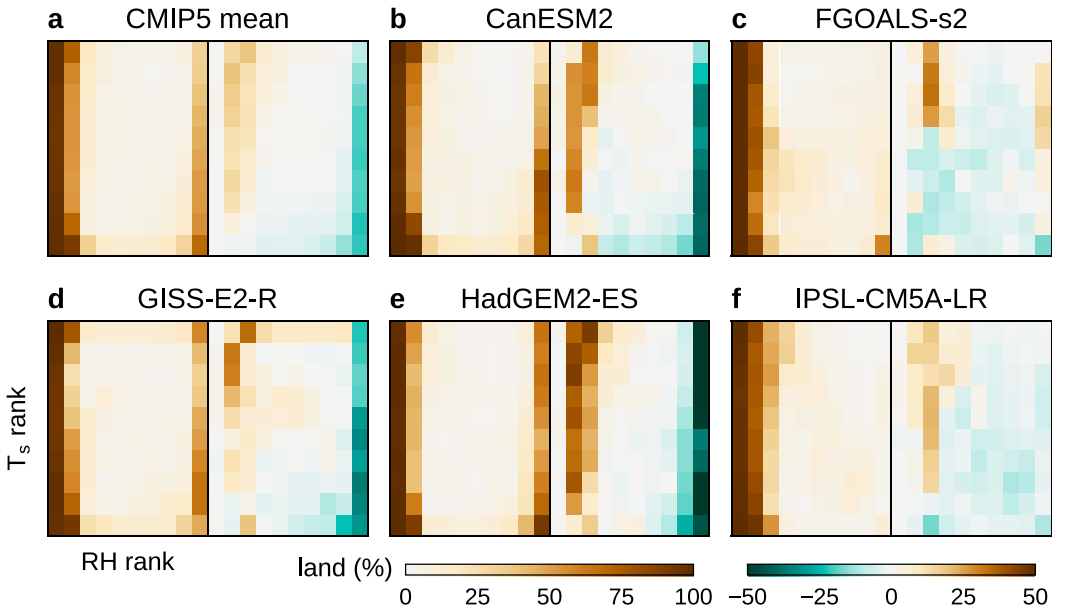

FIG. 3. Fraction of each control composite bin that is land, and change in land fraction when $4\times CO_2$ RH and T_S values are used, shown on the left and right side of each panel, respectively, for (a) the CMIP5 model mean and (b)–(f) our five marker models. In the majority of models, land is most common in the highest and lowest RH bins. FGOALS-s2 and IPSL-CM5A-LR are exceptions, where land is mostly present in the lowest RH bins only. Under climate change, most models show a strong shift of land from high to low RH rank and some shift of land from low to high T_S rank. RH shifts in FGOALS-s2 and IPSL-CM5A-LR are necessarily weaker, as little land starts at high RH.

show good overall agreement with GCM-simulated changes in HadGEM2-ES ($r = 0.78$) and CanESM2 ($r = 0.78$), reasonable agreement in GISS-E2-R ($r = 0.65$) and the CMIP5 mean ($r = 0.59$), and poor agreement in IPSL-CM5A-LR ($r = 0.15$) and especially FGOALS-s2 ($r = -0.05$). Compositing scheme performance varies regionally, however, particularly over important-to-predict land. Despite strong correlation overall, the scheme overestimates precipitation reductions over South America in HadGEM2-ES and Africa for HadGEM2-ES and CanESM2. Although overall correlation is weaker for GISS-E2-R, the scheme performs relatively well over land, with much of the mismatch to GCM results over the Pacific Ocean.

Summary correlation and OLS regression of predicted on GCM-simulated values are shown for all GCMs in the left panels of Figs. 7 and 8, respectively. (Numbers are shown in Table S2.) Note that 13 of 22 predictions show correlations of 0.5 or better, indicating that the shape of the predicted response is about as good as that for GISS-E2-R or better, but all but HadGEM2-ES and ACCESS1.0 show OLS slopes less than and inconsistent with 1, indicating that the size of the response is underestimated. The regression coefficient for CMIP5 mean data is 0.46 ± 0.11; the mean of the coefficients for each GCM is 0.39 ± 0.50, where the error is 2 standard deviations of the spread of the individual GCM coefficients, indicating a wide range of responses across models. Improved predictions are made if we use our mean precipitation change scaled composites to predict $4\times CO_2$ precipitation amounts in each bin, ΔP_{scaled}, reflected by improvements in correlations in almost all models (19 of 22 have correlations greater than 0.5; see Fig. 7, middle panel). The CMIP5 mean slope coefficient is 0.73 ± 0.12; the mean of the coefficients for each GCM is 0.54 ± 0.57. Because unforced internal variability plays a role in precipitation amounts, we rerun our analysis using five separate 30-yr control segments for each of our five marker GCMs. This does produce some changes in correlation and regression coefficients but does not have a qualitative effect on our conclusions. We therefore do not discuss the effects of variability further in the main text. Instead, details are given in the supplemental information (section 2 therein). We note, however, that the effect of internal variability would probably be more important for lower forcing, more realistic scenarios (e.g., Deser et al. 2012).

The composites predict shifts in precipitation when grid boxes change RH and T_S ranking under climate change. In practice, the largest shifts arise when grid boxes change RH ranking, because a small change in RH value can cause a large change in RH ranking and a corresponding large precipitation change. This is important in HadGEM2-ES, CanESM2, and GISS-E2-R, where large numbers of land grid boxes shift from high

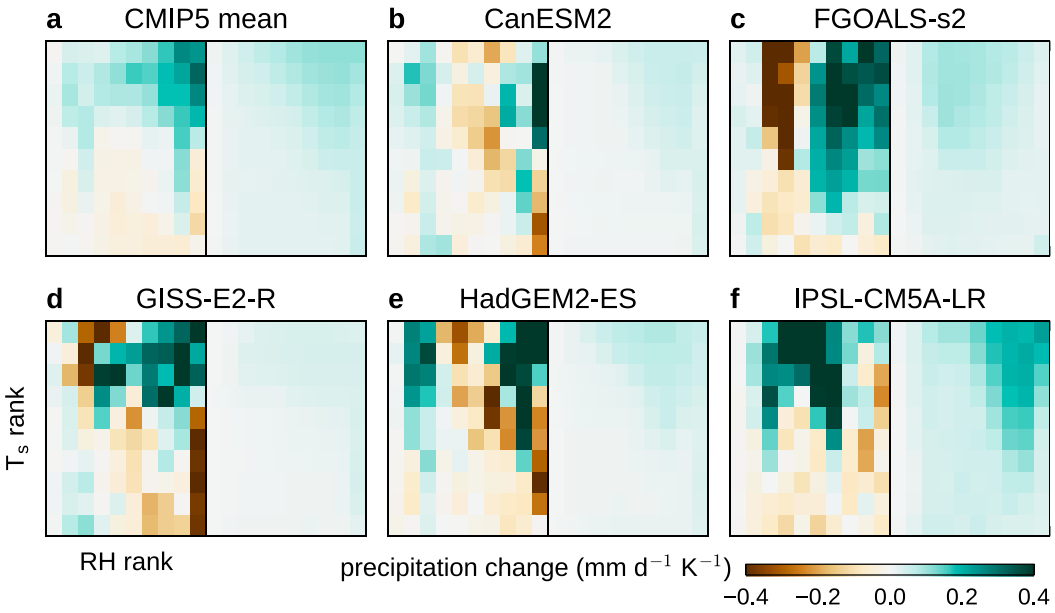

FIG. 4. 4×CO_2–control GCM-simulated changes, and scaling-predicted precipitation composite values, shown on the left and right side of each panel, respectively (mm day^{-1} K^{-1} tropical mean warming), for (a) the CMIP5 model mean and (b)–(f) our five marker models. The CMIP5 mean and the individual GCMs show a "rich-get-richer" response that is partially represented by the scaling prediction. However, the GCM-simulated changes show larger changes with more structure and some strong reductions, particularly in drier regions.

RH ranking to low RH ranking (Fig. 3 right-hand side of panels). This predicts decreases in precipitation over land (much of it over South America) and compensating increases over ocean that are largely replicated by GCM-simulated changes in these models. The CMIP5 mean indicates that these results are fairly common across models. However, this effect is necessarily weak in IPSL-CM5A-LR and FGOALS-s2, because relatively few land grid boxes have high RH rank in the control run. Large shifts over land from high RH to low RH rank therefore cannot occur and shifts of precipitation from land to ocean are not predicted by the composites. It is also largely the case that shifts in precipitation from land to ocean are not simulated by these GCMs, although the weakness of the composite predictions in reproducing GCM simulated changes makes it inappropriate to draw strong conclusions. We note, however, that our composite predictions successfully predict the modest land–ocean shifts in models such as GFDL-ESM2M and MIROC-ESM. These modest shifts are associated with modest declines in land RH rankings. Meridional mean, zonal mean, and map plots may be found in the supplemental information (section 1 therein) for all GCMs.

Finally, we calculate correlations and OLS slopes for the perturbed case where 4×CO_2 predictions are made using 4×CO_2 precipitation amounts composited on 4×CO_2 RH–T_S bins, ΔP_{pert}, as a consistency check. Recall that this is the maximum accuracy possible with our method, because control and perturbed RH and T_S and control precipitation values are known. Interestingly, predictions for some models—MIROC5 in particular—are still very poor, indicating that meridional mean tropical precipitation amounts are poorly classified in terms of RH and T_S in these GCMs. (Zonal and geographical predictions for MIROC5 are nevertheless quite good, indicating that it is the meridional mean in particular that cannot be predicted; see Figs. S6 and S7.) Similar to the scaled case, 19 of 22 GCMs show correlations greater than 0.5 (Fig. 7, right panel). The slope coefficients show a modest improvement compared with the scaled case: the CMIP5 mean slope coefficient is 0.78 ± 0.09, and the mean of the coefficients for each GCM is 0.59 ± 0.42. (Full numbers are shown in Table S2.)

To focus attention on land–ocean shifts in precipitation, Fig. 9 shows land mean changes in GCM-modeled precipitation against land mean RH rank change across Amazonia, tropical Africa, and the Maritime Continent. Large reductions in Amazonian precipitation occur in some models that are associated with large reductions in RH rank that correspond to RH reductions of about 3% K^{-1} (typically the largest across the tropics). HadGEM2-ES and ACCESS-1.0 are outliers in Amazonia, showing large decreases in RH of about 6%–7% K^{-1}. These large RH decreases produce predictions of large Amazonian precipitation decreases in these models that tend to

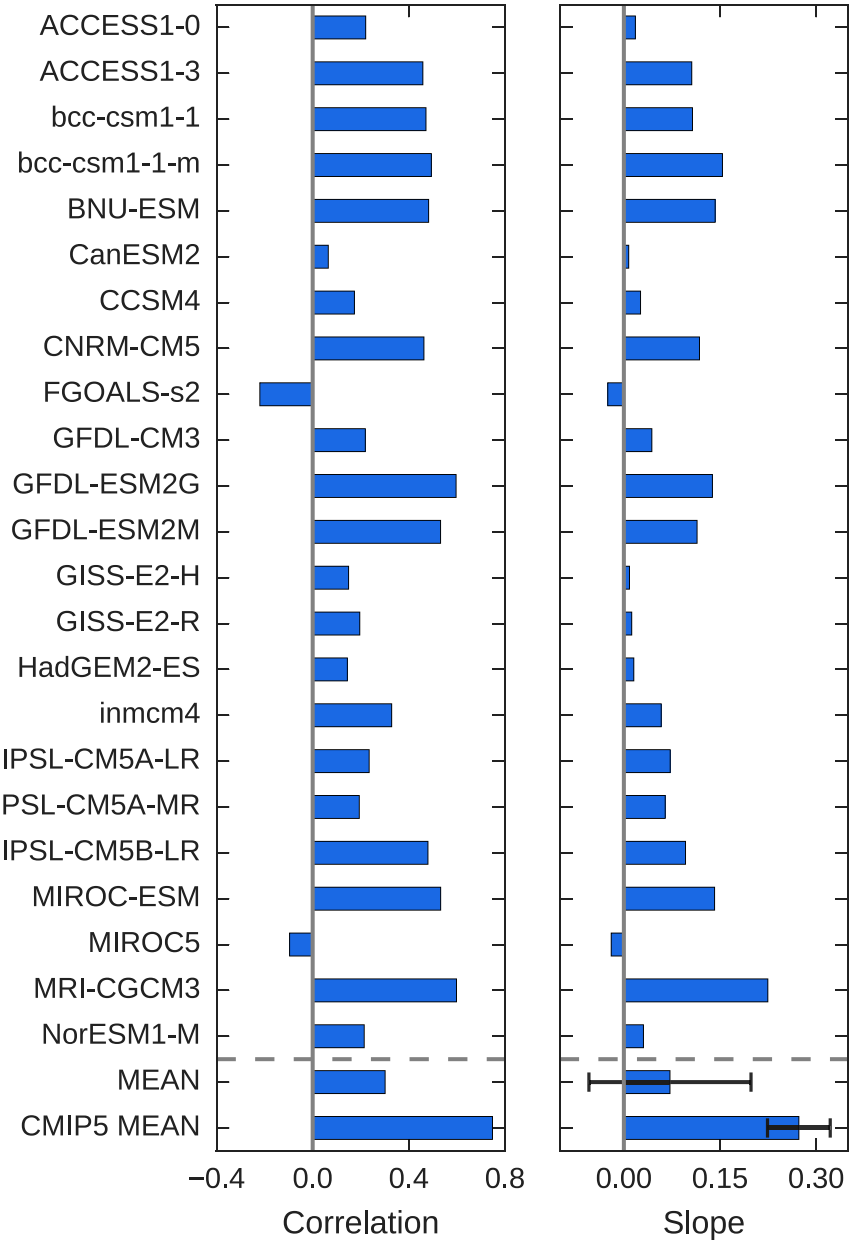

FIG. 5. (left) Correlations and (right) ordinary least squares regression slopes for GCM-simulated changes for each GCM against total "thermodynamic" and "weakening" changes predicted by scaling each control RH–T_S composite bin by mean precipitation change per K warming against GCM-simulated changes for each GCM and the CMIP5 mean. MEAN is the mean correlation and slope across models. The whisker on the MEAN slope bar is the mean error across the individual GCMs taken as two standard deviations of the fit of the OLS slope parameter. CMIP5 MEAN is the correlation and slope for the CMIP5 meridional mean. The whisker on the CMIP5 MEAN OLS slope bar is two standard deviations of the fit for the CMIP5 mean.

overestimate simulated precipitation decreases (see Fig. 6 and Fig. S5). A number of models also show increases in Amazonian precipitation, associated with no change or small positive change in RH rank. Small changes in tropical African precipitation are associated with small changes in RH rank. Where reductions in precipitation occur, these correspond to RH reductions of about 1% K^{-1}. Over the Maritime Continent, a number of models show either large positive or large negative changes in precipitation that are not associated with any change in RH

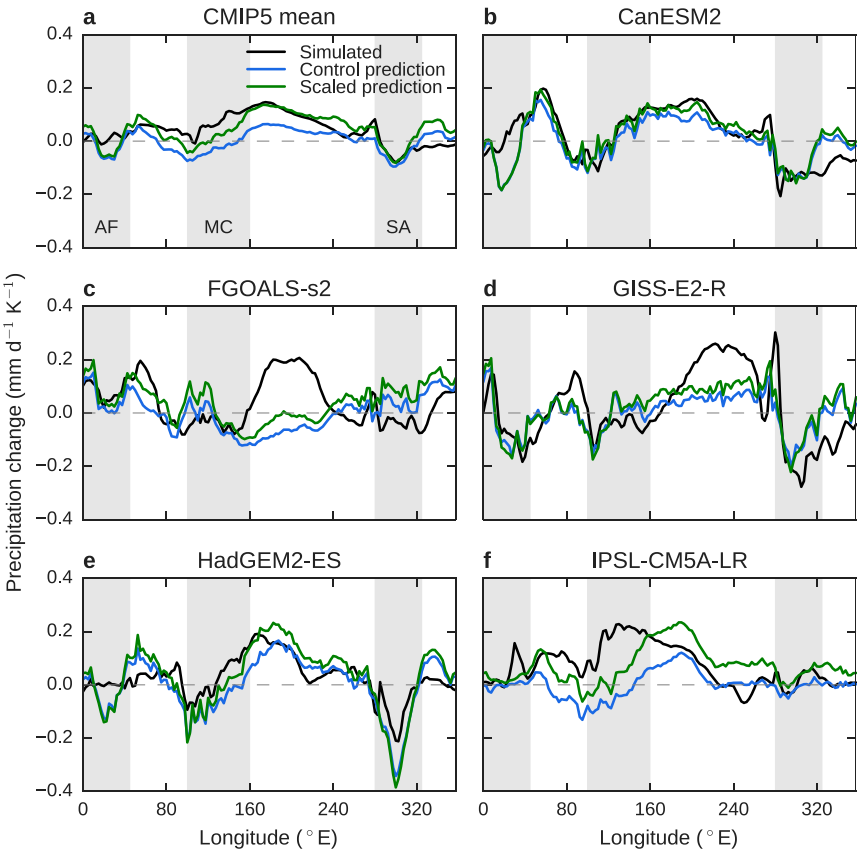

FIG. 6. The 4×CO_2–control changes in meridional mean precipitation simulated by GCMs (black), shifts predicted by the control RH–T_S precipitation composite (blue), and changes predicted by the scaled RH–T_S precipitation composite (green), in mm day^{-1} K^{-1} tropical mean warming, for (a) the CMIP5 model mean and (b)–(f) our five marker models. Gray vertical bands represent the longitudinal extents of Africa (AF), the Maritime Continent (MC), and South America (SA). Good agreement between composite and simulated values is found for HadGEM2-ES ($r = 0.78$) and CanESM2 ($r = 0.78$); reasonable agreement is found for GISS-E2-Rv ($r = 0.65$); little agreement is found for IPSL-CM5A-LR ($r = 0.15$) and FGOALS-s2 ($r = -0.05$).

rank. This occurs despite RH–T_S composite predictions of precipitation change being in general no worse than elsewhere (see Figs. 6 and S5). This may be because both GCM-simulated values and composite predictions show a dipole-like response with compensating increases and reductions across the Maritime Continent for many models, in contrast to the more spatially uniform decrease seen over Amazonia. Maps of RH change per Kelvin are shown in Fig. S9.

In summary, we find that zonally asymmetric tropical precipitation change is quite well associated with near-surface RH and T_S change in more than half of CMIP5 GCMs, but poorly related in a few others. There is little skill in predicting precipitation changes in composite bins when changes are estimated by scaling precipitation amounts by mean tropical precipitation change, but using the scaled composite does offer improved predictions of meridional mean precipitation change. This implies that errors introduced by our inability to predict changes in the composites themselves are second order when it comes to predicting geographical precipitation changes. A feature of many predicted and GCM-simulated changes is a shift of precipitation from land to ocean associated with decreases in RH over land that produce large decreases in land RH rank. A continental analysis shows that in models where land precipitation is reduced, the largest changes typically occur over Amazonia.

5. Land precipitation predictions without knowledge of land humidity change

We now discuss the possibility for predictions of land tropical precipitation change when we do not know changes in land humidity in the perturbed simulation.

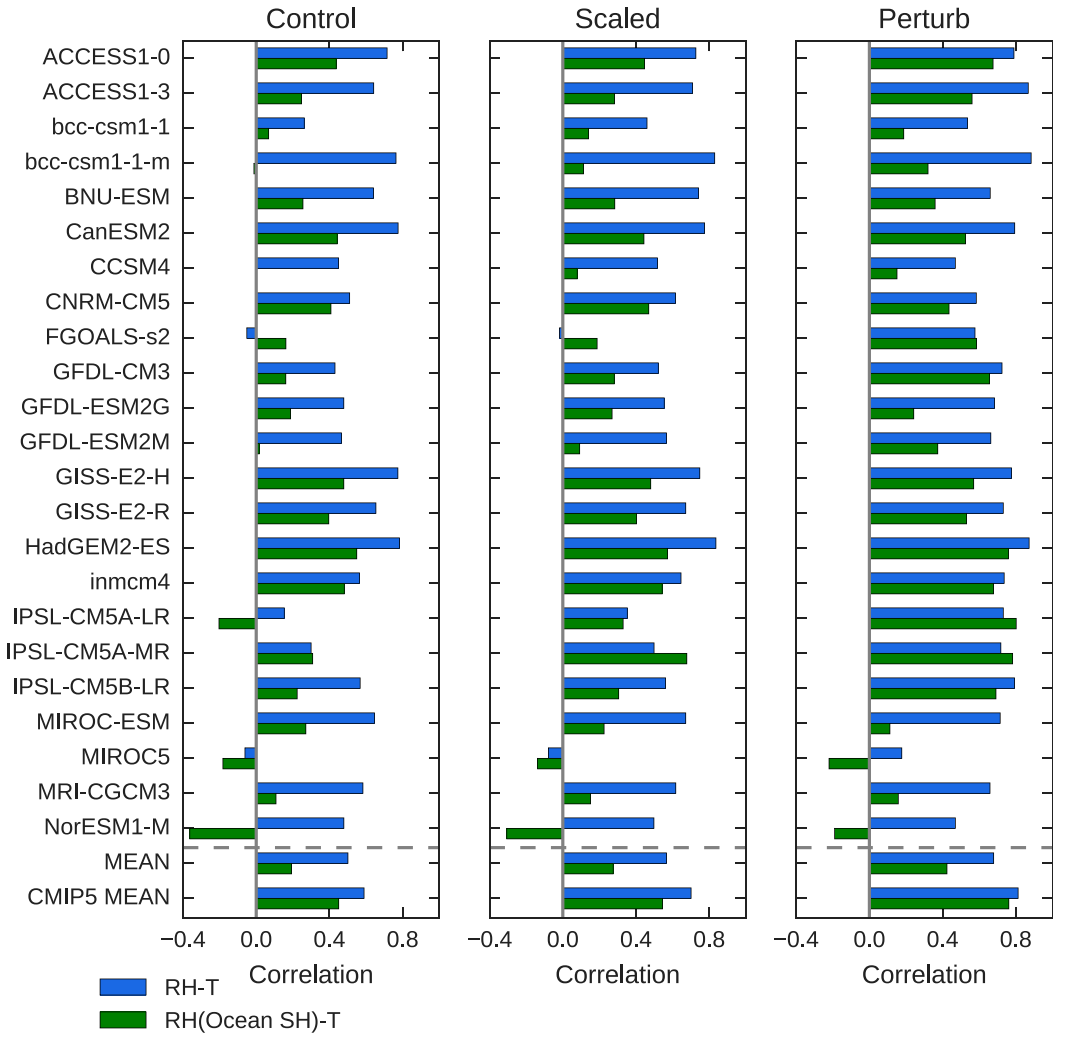

FIG. 7. Correlations for composite predicted meridional mean precipitation changes against GCM-simulated changes, for (left) control composites, (middle) scaled composites, and (right) perturbed composites. The blue bars are for the RH–T_S composites with known RH and T_S change; the green bars are for the RH–T_S composites when land RH is estimated via ocean SH scaling. MEAN is the mean correlation across models. CMIP5 MEAN is the correlation for the CMIP5 meridional mean.

Inspired by Rowell and Jones (2006), Byrne and O'Gorman (2016) and Chadwick et al. (2016) demonstrated that changes in GCM-simulated land near surface SH can be estimated by assuming the same fractional change as ocean mean SH. Recognizing that this may be a first step toward a prognostic theory of tropical precipitation shifts, we re-estimate changes in precipitation using our RH–T_S composites, but this time estimating land SH change as being in proportion to mean ocean SH change within the same latitude circle, following Chadwick et al. (2016). Ocean SH change we set to mean change for each latitude circle. We refer to this as "ocean SH scaling."

We find changes in $4\times CO_2$–control precipitation for our marker models shown in Fig. 10. Agreement between scaled, ΔP_{scaled}, and simulated responses is degraded for all GCMs compared with the case where land RH change is treated as known, Fig. 6. Correlation and regression coefficients for the meridional mean are shown as green bars in Figs. 7 and 8; numbers are given in Table S4. For the scaled composites, only 3 of 22 correlations are above 0.5; 7 are above 0.4. Also, 15 of 22 cases show regression coefficients that are positive and inconsistent with zero indicating that the majority of ocean SH scaling predictions show some relationship with GCM simulated values. It should be noted, though, that all regression coefficients are significantly less than 1, meaning that precipitation change is underestimated in all cases. Nevertheless, we regard our results as an encouraging start.

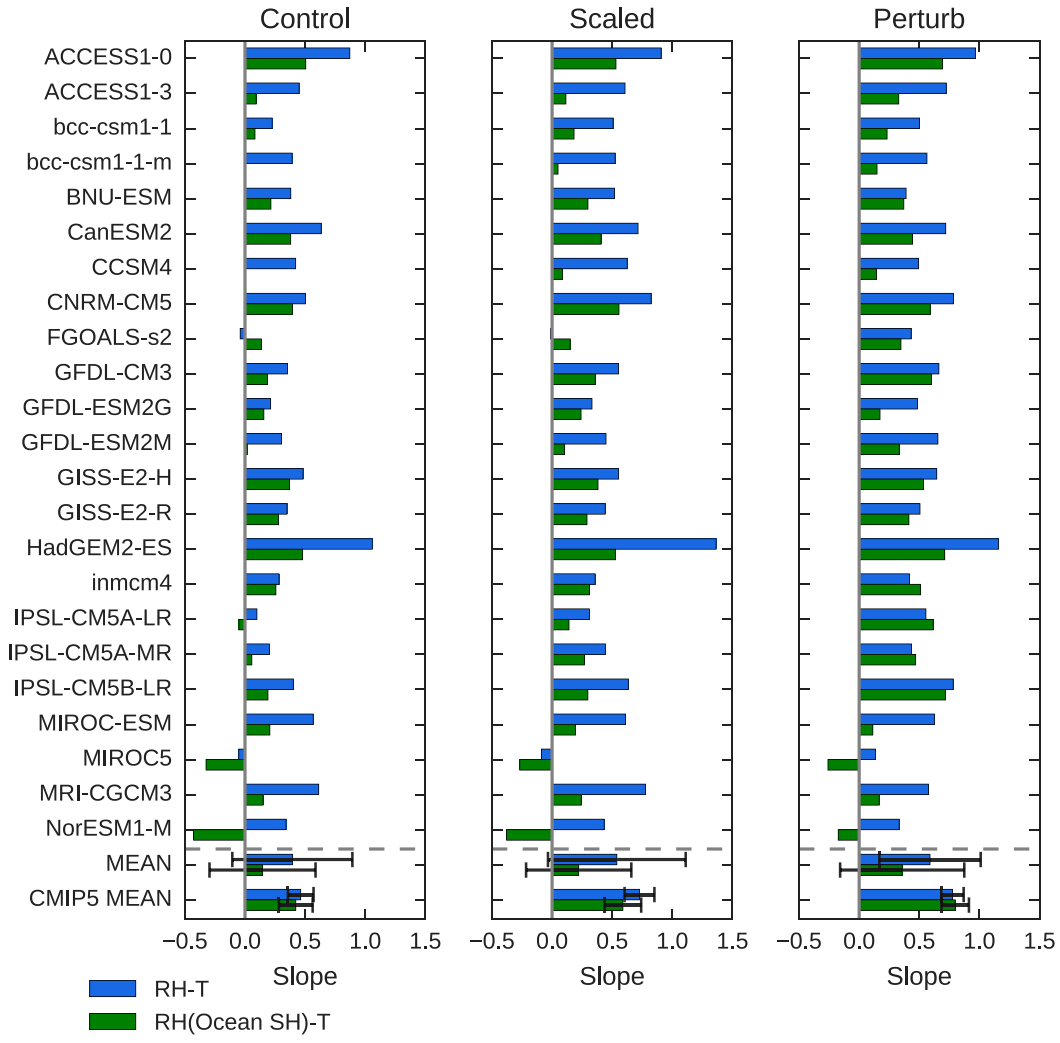

FIG. 8. OLS slopes for composite predicted meridional mean precipitation changes against GCM-simulated changes: (left) control composites, (middle) scaled composites, and (right) perturbed composites. The blue bars are for the RH–T_S composites with known RH and T_S change; the green bars are for the RH–T_S composites when land RH is estimated via ocean SH scaling. MEAN is the slope across models. The whisker on the MEAN slope bar is the mean error across the individual GCMs taken as two standard deviations of the fit of the OLS slope parameter. CMIP5 MEAN is the slope for the CMIP5 meridional mean. The whisker on the CMIP5 MEAN OLS slope bar is two standard deviations of the fit for the CMIP5 mean.

Marker model predictions show skill in predicting simulated reductions in land precipitation, particularly over Amazonia, and compensating increases over ocean. The meridional mean, zonal mean, and maps of predicted against GCM-simulated changes for all models are shown in the supplemental information.

Could our precipitation predictions be improved if we avoid calculation of RH? The success of Byrne and O'Gorman (2016) and Chadwick et al. (2016) in predicting land SH change in a perturbed climate motivates the testing of a simpler compositing scheme that relies on knowledge of SH alone [similar to Biasutti et al. (2006)] and therefore does not rely on estimating RH change. Our alternative scheme groups GCM grid boxes into 10 equal population bins of ascending near-surface SH. No further division of the bins is made. As before, each bin is assigned a precipitation value that is equal to the area-weighted average of the gridbox precipitation in that bin. Precipitation shifts are predicted to be the difference between the control precipitation value associated with the SH ranking in the perturbed run and the control precipitation value associated with the SH value in the control run, equivalent to ΔP_{shift}. We also predict scaled changes that include the effect of thermodynamic and weakening changes by scaling control bin precipitation values by mean precipitation change

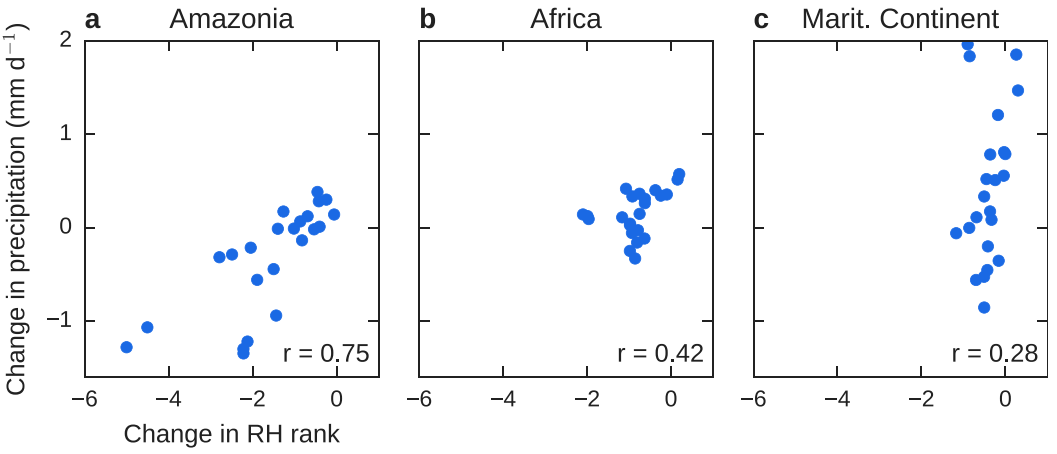

FIG. 9. Mean land precipitation change against mean land change in RH ranking for (a) Amazonia (15°S–5°N, 285°–310°E), (b) Africa (15°S–15°N, 0°–30°E), and (c) the Maritime Continent (15°S–15°N, 100°–150°E). The r values are correlations between precipitation and RH rank changes. Large changes in Amazonian precipitation are associated with large reductions in RH rank of the Amazon. Only small changes in precipitation and RH rank occur over Africa. Large changes in mean precipitation do occur over the Maritime Continent, but these are associated with small changes in RH rank, possibly because GCMs tend to show a dipole-like precipitation response here. These results are total changes, not changes per Kelvin mean tropical warming.

per Kelvin warming, equivalent to ΔP_{scaled}. Some degradation in composite performance is expected, because a range of RH and T_S conditions are plausible for a given SH value.

Full results and a discussion are shown in the supplemental information (section 4 therein). Here we summarize key differences with RH–T_S predictions. Where we allow ourselves to know perturbed GCM simulated RH, T_S, and SH, for scaled composites, 15 of 22 SH predictions remain above 0.5, compared with 19 of 22 for RH–T_S composites. However, where we use ocean SH scaling to predict SH changes, almost no precipitation shifts are predicted by the composites. They are very poor compared even with the ocean SH RH–T_S composites. Why does this happen when ocean SH scaling gives fairly good predictions of future SH and SH composites give fairly good predictions of GCM simulated precipitation change? The issue is that ocean SH scaling changes land SH at the same fractional rate as ocean SH within the same latitude circle, meaning that no grid box may change SH rank with a grid box within the same latitude circle. Hence, regions with higher control SH are generally predicted to remain at higher SH in the $4\times CO_2$ simulation than regions with lower control SH. As a result only very small shifts in precipitation are predicted (not shown).

In summary, ocean SH scaling can be used to provide an indication of changes in tropical regional precipitation in a perturbed climate where T_S change and ocean SH change is known using the RH–T_S compositing method. Predictions are substantially degraded compared with the case where perturbed humidity change is known. However, reductions in Amazonian precipitation are predicted, qualitatively in line with GCM-modeled results. We note that a simplified compositing method based on SH only is also quite successful at reproducing precipitation change if SH change is known, but that it cannot be used with ocean SH scaling because ocean SH scaling cannot properly produce changes in the ranking of grid boxes by SH in the perturbed climate.

6. Discussion

We have presented a scheme that explores the link between tropical surface humidity and temperatures and precipitation changes under climate change. A number of features of CMIP5 GCMs are revealed. The scheme shows some skill in estimating changes in tropical meridional mean precipitation when future RH and T_S changes are known in the majority of models. This suggests that meridional mean changes in RH, T_S, and precipitation may be considered a coupled problem in these GCMs, and that the response is as expected from earlier mean field theory developed from the weak temperature gradient approximation (Sobel and Bretherton 2000). In IPSL-CM5A-LR, MIROC5, and especially FGOALS-s2, precipitation change is poorly related to RH and T_S change. (Interestingly, MIROC5 zonal mean precipitation change is well represented.) This does not mean that these GCMs are wrong. It may be that they simulate physical processes not represented

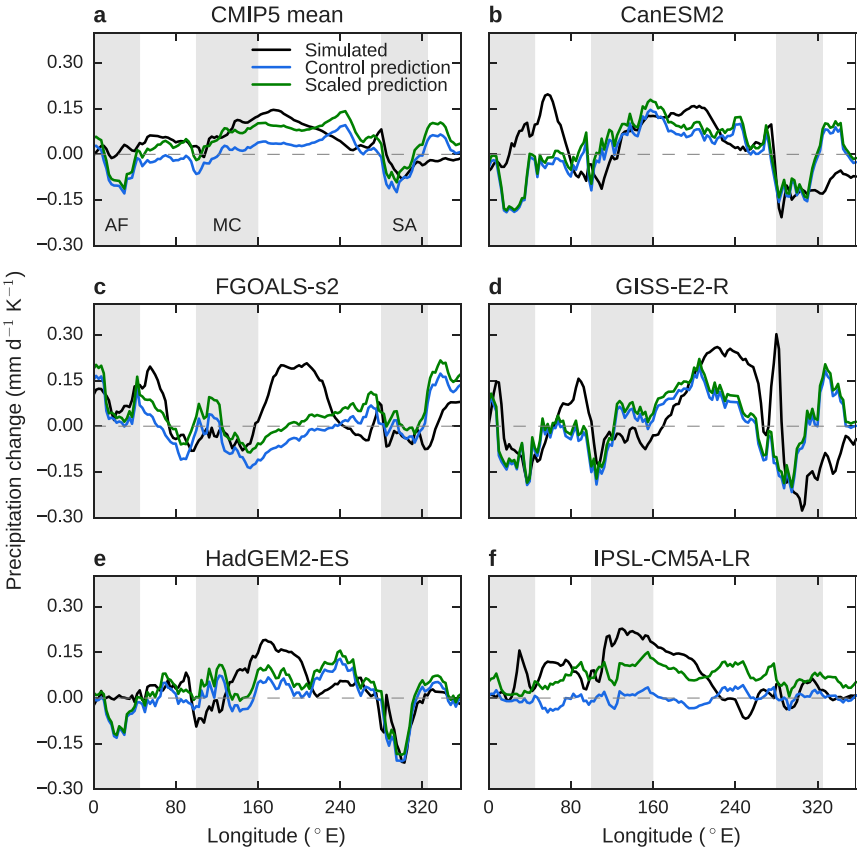

FIG. 10. 4×CO_2–control changes in meridional mean precipitation simulated by GCMs (black), shifts predicted by the control RH–T_S precipitation composite (blue), and changes predicted by the scaled RH–T_S precipitation composite (green) when land SH change is estimated by ocean SH scaling in mm day^{-1} K^{-1} tropical mean warming, for (a) the CMIP5 model mean and (b)–(f) our five marker models. Gray vertical bands represent the longitudinal extents of Africa (AF), the Maritime Continent (MC), and South America (SA). Good agreement between composite and simulated values is found for HadGEM2-ES and CanESM2; reasonable agreement is found for GISS-E2-R; little agreement is found for FGOALS-s2 and IPSL-CM5A-LR.

by other models. This is an important question for future research, because these GCMs do not simulate or only weakly simulate the shift of precipitation from land (particularly South America) to ocean seen in the majority of other CMIP5 GCMs under warming, increasing our uncertainty concerning future climate change.

In GCMs that show shifts in precipitation from land to ocean, the shifts are generally associated with large numbers of land grid boxes, particularly over South America, with high RH ranking in the control run moving to low RH ranking in the perturbed simulation through RH changes of around 3% K^{-1}. This requires that 1) RH bins are quite tightly spaced, meaning that relatively small changes in gridbox RH can lead to large changes in gridbox RH ranking, and 2) large numbers of land grid boxes are found at high RH ranking in the control run. Where these conditions are fulfilled (as in HadGEM2-ES, CanESM2, and GISS-E2-R), the result is that a warming of 5 or 10 K is sufficient to move a large proportion of high RH ranked grid boxes to low RH ranks. GCMs that do not show this behavior, either because land has high RH rank under both control and perturbed conditions (true to some extent of BNU-ESM) or because land has low RH rank under both control and perturbed conditions (as in FGOALS-s2 and IPSL-CM5A-LR), show weak land–ocean shifts in precipitation. A number of models represent in-between cases, such as GFDL-ESM2M and MIROC-ESM, which show some land areas at high RH rank in the control, some decline in land RH rank in the perturbed simulation, and limited land–ocean shifts in precipitation. These relationships motivate two immediate goals of our future work. First, it must determine whether observed interannual climate variability shows coupled

changes in RH, T_S, and precipitation. Second, if this is the case, then it must discover whether or not the real world is close to a threshold that could lead to a large reduction in precipitation over some land areas under tropical warming expected in the twenty-first century. The CO_2 quadrupling simulations that we analyzed are idealized, but not incomparable to end-of-century warming in strongly forced future scenarios such as RCP8.5 (Collins et al. 2013; Chadwick 2016). We therefore expect our results to be relevant to projections of climate change, although unexplored issues concerning direct heating of the atmosphere by aerosol forcing will need to be addressed. We also note that other recent work has emphasized the importance of radiative feedbacks and their impact on the surface and atmospheric energy budget for the hydrological cycle (Maroon et al. 2016; Oueslati et al. 2016). Where these feedbacks are not simply coupled to surface humidity and temperature change, our compositing scheme may perform poorly.

Improved precipitation change predictions were obtained when our RH–T_S composites were scaled by tropical mean precipitation change. This represents an estimate of the combined thermodynamic–weakening change when surface SH and tropical circulation in every grid box change in proportion to their climatological values, similar to the method of Chadwick et al. (2013). Although geographical precipitation predictions are improved, the change in the composites themselves is poorly represented—these contain much stronger and more complex changes than we can predict, suggesting that unrecognized processes control composite change, or that our compositing method does not fully remove shifts. One possible issue is that we have composited land and ocean precipitation together, a choice usually avoided in other composite studies of the tropics or other simple models of tropical precipitation (e.g., Lindzen and Nigam 1987; Neelin and Held 1987; Bretherton et al. 2004; Biasutti et al. 2006) because land precipitation is sensitive to different processes than ocean precipitation (e.g., Eltahir 1998; Betts 2004; Fasullo 2012). Hence, it may be that differences in the geographical regions that contribute to each composite bin in the perturbed and control climate contribute to composite changes, particularly if the fraction of land in the bin changes significantly.

Building a useful compositing scheme means finding a minimum set of information that can be related to precipitation amounts with sufficient accuracy. We chose RH and T_S because these variables are important to atmospheric convection and are potentially observable, and because they are ones for which some progress has been made in predicting changes in future climates. Regarding the last point, previous work has shown that SH change over ocean maintains approximately constant RH as T_S increases, and SH changes over land tend to show the same fractional increases in SH as over ocean (Byrne and O'Gorman 2016; Chadwick et al. 2016). We have referred to this as ocean SH scaling. A problem, however, is that although ocean SH scaling captures changes in perturbed SH quite well, we do see substantial degradations in our compositing scheme GCM precipitation predictions. The principal issue is that ocean SH scaling cannot interchange the SH rank of two GCM grid boxes in the same latitude circle. This difficulty is highlighted when we try to predict shifts in rainfall in a perturbed climate using ocean SH scaling in a simple one-dimensional SH compositing scheme that avoids the need for separate estimates of RH and T_S. The SH scheme is only somewhat less accurate than the RH–T_S scheme when values of future temperature and humidity change are known. When ocean SH scaling is employed to estimate SH change, however, the SH scheme fails to predict almost any changes in precipitation at all because grid boxes within a given latitude circle must change SH rank to produce substantial meridional mean precipitation changes.

It is also important to note that the ocean SH scaling response assumes that there are no changes in the location of circulation. This is incompatible with our precipitation compositing schemes, which arise from a picture in which the most intense precipitation and regions of atmospheric convergence are collocated and move together under climate change. Ocean SH scaling also neglects at least some effects of land–atmosphere feedbacks, which may for example arise from shifts in precipitation themselves that then couple to changes in near-surface humidity (Eltahir 1998; Betts 2004; Betts et al. 2004; Berg et al. 2016). This may explain why even where our ocean SH scaled RH–T_S composites are relatively successful, they always underestimate precipitation response. It is likely that simultaneous estimates of precipitation and land surface humidity are needed. A potential avenue for research might be to build a simple model of the land surface heat budget (e.g., Zeng and Neelin 1999).

Nevertheless, we regard our ocean SH scaling results as a promising start for which further improvements may be possible in future if the above issues can be overcome. Given that RH in the oceanic boundary layer remains quite constant under climate change (our GCMs mostly show a small increase) and that changes in tropical ocean T_S are fairly uniform, changes in land SH per Kelvin might be estimated from the climatology and changes in sea surface temperatures. If this is combined with predictions of land T_S for a given ocean T_S by

equating values of equivalent potential temperature, θ_E, over land and ocean (Byrne and O'Gorman 2013), then estimates of changes in land–sea contrast of RH and T_S can be found in principle. Obtaining estimates of tropical precipitation change would then require knowledge of climatology and ocean T_S change only.

7. Summary

We have combined precipitation compositing and mean field theory methods from previous work to relate changes in CMIP5 general circulation model (GCM) simulated tropical precipitation when atmospheric CO_2 concentration is quadrupled. A compositing method is used to relate precipitation amounts at a given location to values of local relative humidity (RH) and surface temperature T_S. Changes in precipitation at a given location in the perturbed climate are then associated with changes in the RH and T_S relative to other locations so that precipitation change depends principally on change of the RH and T_S rank of that location in accordance with the weak temperature gradient approximation.

Land–sea "shifts" in patterns of precipitation that dominate tropical precipitation change in most CMIP5 GCMs are found to be associated largely with decreases in the RH rank of land grid boxes, which are due to decreases in land RH noted by previous work. (The dominant response over ocean only has been shown to be associated with changes in sea surface temperature; Xie et al. 2010; Zhang and Li 2016b). Other recent work has begun to develop quantitative predictions of changes in land humidity and temperature, suggesting that it may be possible to develop a prognostic theory of precipitation change in future. We combined our compositing method with GCM-simulated T_S and RH changes predicted from the method of Byrne and O'Gorman (2016) and Chadwick et al. (2016), which we call ocean SH scaling. The method shows some skill in predicting the sense of future tropical precipitation change, but magnitudes of changes are too small in all cases, probably because radiative and land–atmosphere feedbacks are neglected. We find that a simpler scheme that depends only on knowledge of SH can also predict shifts in precipitation in most GCMs when SH change is known. However, when it is coupled with ocean SH scaling, it fails to make adequate predictions.

A distinctive feature of our results is that many CMIP5 GCM control runs are near a threshold at which reductions of around 10% in land RH are sufficient to cause large reductions in the rank of land gridpoint RH and therefore large reductions in land precipitation, especially over Amazonia. GCMs that are not near this threshold do not in general produce substantial land to ocean shifts in precipitation. Our future work will therefore focus on discovering whether or not real-world precipitation change is associated with surface humidity and temperature change—it is not in some GCMs—and whether the real world is near the land RH threshold.

Acknowledgments. We are grateful to Richard Allan, whose suggestions substantially improved results. We acknowledge the World Climate Research Programme's Working Group on Coupled Modelling, which is responsible for CMIP, and we thank the climate modeling groups (listed in Table 1) for producing and making available their model output. For CMIP the U.S. Department of Energy's Program for Climate Model Diagnosis and Intercomparison provides coordinating support and led development of software infrastructure in partnership with the Global Organization for Earth System Science Portals. We thank the JASMIN and CEDA team for making available the JASMIN computing resource (Lawrence et al. 2013). FHL was part supported by the UK-China Research and Innovation Partnership Fund through the Met Office Climate Science for Service Partnership (CSSP) China as part of the Newton Fund; AJF was supported by the NERC PROBEC Project NE/K016016/1; RC was supported by the Newton Fund through the Met Office CSSP Brazil.

REFERENCES

Allan, R. P., 2012: Regime dependent changes in global precipitation. *Climate Dyn.*, **39**, 827–840, doi:10.1007/s00382-011-1134-x.

——, 2014: Climate change: Dichotomy of drought and deluge. *Nat. Geosci.*, **7**, 700–701, doi:10.1038/ngeo2243.

Andrews, T., J. M. Gregory, P. M. Forster, and M. J. Webb, 2012: Cloud adjustment and its role in CO_2 radiative forcing and climate sensitivity: A review. *Surv. Geophys.*, **33**, 619–635, doi:10.1007/s10712-011-9152-0.

Bao, Q., and Coauthors, 2013: The Flexible Global Ocean–Atmosphere–Land system model, spectral version 2: FGOALS-s2. *Adv. Atmos. Sci.*, **30**, 561–576, doi:10.1007/s00376-012-2113-9.

Bentsen, M., and Coauthors, 2013: The Norwegian Earth System Model, NorESM1-M—Part 1: Description and basic evaluation. *Geo. Model Dev.*, **6**, 687–720, doi:10.5194/gmd-6-687-2013.

Berg, A., and Coauthors, 2016: Land–atmosphere feedbacks amplify aridity increase over land under global warming. *Nat. Climate Change*, **6**, 869–874, doi:10.1038/nclimate3029.

Betts, A. K., 2004: Understanding hydrometeorology using global models. *Bull. Amer. Meteor. Soc.*, **85**, 1673–1688, doi:10.1175/BAMS-85-11-1673.

Betts, R. A., P. M. Cox, M. Collins, P. P. Harris, C. Huntingford, and C. D. Jones, 2004: The role of ecosystem–atmosphere interactions in simulated Amazonian precipitation decrease and forest dieback under global climate warming. *Theor. Appl. Climatol.*, **78**, 157–175, doi:10.1007/s00704-004-0050-y.

Bi, D., and Coauthors, 2013: The ACCESS coupled model: Description, control climate and evaluation. *Aust. Meteor. Oceanogr. J.*, **63**, 41–64.

Biasutti, M., A. H. Sobel, and Y. Kushnir, 2006: AGCM precipitation biases in the tropical Atlantic. *J. Climate*, **19**, 935–958, doi:10.1175/JCLI3673.1.

Blossey, P. N., C. S. Bretherton, and M. C. Wyant, 2009: Subtropical low cloud response to a warmer climate in a superparameterized climate model. Part II: Column modeling with a cloud resolving model. *J. Adv. Model. Earth Syst.*, **1** (8), doi:10.3894/JAMES.2009.1.8.

Bony, S., G. Bellon, D. Klocke, S. Sherwood, S. Fermepin, and S. Denvil, 2013: Robust direct effect of carbon dioxide on tropical circulation and regional precipitation. *Nat. Geosci.*, **6**, 447–451, doi:10.1038/ngeo1799.

Bordoni, S., and T. Schneider, 2008: Monsoons as eddy-mediated regime transitions of the tropical overturning circulation. *Nat. Geosci.*, **1**, 515–519, doi:10.1038/ngeo248.

Bretherton, C. S., M. E. Peters, and L. E. Back, 2004: Relationships between water vapor path and precipitation over the tropical oceans. *J. Climate*, **17**, 1517–1528, doi:10.1175/1520-0442(2004)017<1517:RBWVPA>2.0.CO;2.

Byrne, M. P., and P. A. O'Gorman, 2013: Link between land–ocean warming contrast and surface relative humidities in simulations with coupled climate models. *Geophys. Res. Lett.*, **40**, 5223–5227, doi:10.1002/grl.50971.

——, and ——, 2016: Understanding decreases in land relative humidity with global warming: Conceptual model and GCM simulations. *J. Climate*, **29**, 9045–9061, doi:10.1175/JCLI-D-16-0351.1.

Caldeira, K., and N. P. Myhrvold, 2013: Projections of the pace of warming following an abrupt increase in atmospheric carbon dioxide concentration. *Environ. Res. Lett.*, **8**, 034039, doi:10.1088/1748-9326/8/3/034039.

Chadwick, R., 2016: Which aspects of CO_2 forcing and SST warming cause most uncertainty in projections of tropical rainfall change over land and ocean? *J. Climate*, **29**, 2493–2509, doi:10.1175/JCLI-D-15-0777.1.

——, I. Boutle, and G. Martin, 2013: Spatial patterns of precipitation change in CMIP5: Why the rich do not get richer in the tropics. *J. Climate*, **26**, 3803–3822, doi:10.1175/JCLI-D-12-00543.1.

——, P. Good, T. Andrews, and G. Martin, 2014: Surface warming patterns drive tropical rainfall pattern responses to CO_2 forcing on all timescales. *Geophys. Res. Lett.*, **41**, 610–615, doi:10.1002/2013GL058504.

——, ——, and K. Willett, 2016: A simple moisture advection model of specific humidity change over land in response to SST warming. *J. Climate*, **29**, 7613–7632, doi:10.1175/JCLI-D-16-0241.1.

Chiang, J. C. H., C. Chang, and M. Wehner, 2013: Long-term behavior of the Atlantic interhemispheric SST gradient in the CMIP5 historical simulations. *J. Climate*, **26**, 8628–8640, doi:10.1175/JCLI-D-12-00487.1.

Chou, C., and J. D. Neelin, 2004: Mechanisms of global warming impacts on regional tropical precipitation. *J. Climate*, **17**, 2688–2701, doi:10.1175/1520-0442(2004)017<2688:MOGWIO>2.0.CO;2.

Collins, M., and Coauthors, 2013: Long-term climate change: Projections, commitments and irreversibility. *Climate Change 2013: The Physical Science Basis*, T. Stocker et al., Eds., Cambridge University Press, 1029–1136.

Dal Gesso, S., J. J. van der Dussen, A. P. Siebesma, S. R. de Roode, I. A. Boutle, Y. Kamae, R. Roehrig, and J. Vial, 2015: A single-column model intercomparison on the stratocumulus representation in present-day and future climate. *J. Adv. Model. Earth Syst.*, **7**, 617–647, doi:10.1002/2014MS000377.

Deser, C., A. S. Phillips, V. Bourdette, and H. Teng, 2012: Uncertainty in climate change projections: The role of internal variability. *Climate Dyn.*, **38**, 527–546, doi:10.1007/s00382-010-0977-x.

Donner, L. J., and Coauthors, 2011: The dynamical core, physical parameterizations, and basic simulation characteristics of the atmospheric component AM3 of the GFDL global coupled model CM3. *J. Climate*, **24**, 3484–3519, doi:10.1175/2011JCLI3955.1.

Dufresne, J. L., and Coauthors, 2013: Climate change projections using the IPSL-CM5 Earth system model: From CMIP3 to CMIP5. *Climate Dyn.*, **40**, 2123–2165, doi:10.1007/s00382-012-1636-1.

Dunne, J. P., and Coauthors, 2012: GFDL's ESM2 global coupled climate–carbon Earth system models. Part I: Physical formulation and baseline simulation characteristics. *J. Climate*, **25**, 6646–6665, doi:10.1175/JCLI-D-11-00560.1.

Eltahir, E. A. B., 1998: A soil moisture–rainfall feedback mechanism: 1. Theory and observations. *Water Resour. Res.*, **34**, 765–776, doi:10.1029/97WR03499.

Emori, S., and S. J. Brown, 2005: Dynamic and thermodynamic changes in mean and extreme precipitation under changed climate. *Geophys. Res. Lett.*, **32**, L17706, doi:10.1029/2005GL023272.

Fasullo, J. T., 2012: A mechanism for land–ocean contrasts in global monsoon trends in a warming climate. *Climate Dyn.*, **39**, 1137–1147, doi:10.1007/s00382-011-1270-3.

Ferraro, A. J., F. H. Lambert, M. Collins, and G. M. Miles, 2015: Physical mechanisms of tropical climate feedbacks investigated using temperature and moisture trends. *J. Climate*, **28**, 8968–8987, doi:10.1175/JCLI-D-15-0253.1.

Frieler, K., M. Meinshausen, T. Schneider von Deimling, T. Andrews, and P. Forster, 2011: Changes in global-mean precipitation in response to warming, greenhouse gas forcing and black carbon. *Geophys. Res. Lett.*, **38**, L04702, doi:10.1029/2010GL045953.

Gent, P. R., and Coauthors, 2011: The Community Climate System Model version 4. *J. Climate*, **24**, 4973–4991, doi:10.1175/2011JCLI4083.1.

Good, P., B. B. B. Booth, R. Chadwick, E. Hawkins, A. Jonko, and J. A. Lowe, 2016: Large differences in regional precipitation change between a first and second 2 K of global warming. *Nat. Commun.*, **7**, 13667, doi:10.1038/ncomms13667.

Hawkins, E., M. Joshi, and D. Frame, 2014: Wetter then drier in some tropical areas. *Nat. Climate Change*, **4**, 646–647, doi:10.1038/nclimate2299.

Held, I. M., and B. J. Soden, 2006: Robust responses of the hydrological cycle to global warming. *J. Climate*, **19**, 5686–5699, doi:10.1175/JCLI3990.1.

Hwang, Y., D. M. W. Frierson, and S. M. Kang, 2013: Anthropogenic sulfate aerosol and the southward shift of tropical precipitation in the late 20th century. *Geophys. Res. Lett.*, **40**, 2845–2850, doi:10.1002/grl.50502.

Ji, D., and Coauthors, 2014: Description and basic evaluation of Beijing Normal University Earth System Model (BNU-ESM) version 1. *Geosci. Model Dev.*, **7**, 2039–2064, doi:10.5194/gmdd-7-1601-2014.

Johnson, N. C., and S.-P. Xie, 2010: Changes in the sea surface temperature threshold for tropical convection. *Nat. Climate Change*, **3**, 842–845, doi:10.1038/ngeo1008.

Krejci, R., J. Ström, M. de Reus, and W. Sahle, 2005: Single particle analysis of the accumulation mode aerosol over the northeast Amazonian tropical rain forest, Surinam, South America. *Atmos. Chem. Phys.*, **5**, 3331–3344, doi:10.5194/acp-5-3331-2005.

Lambert, F. H., and P. C. Taylor, 2014: Regional variation of the tropical water vapor and lapse rate feedbacks. *Geophys. Res. Lett.*, **41**, 7634–7641, doi:10.1002/2014GL061987.

——, M. J. Webb, and M. M. Joshi, 2011: The relationship between land–ocean surface temperature contrast and radiative forcing. *J. Climate*, **24**, 3239–3256, doi:10.1175/2011JCLI3893.1.

Lawrence, B. N., and Coauthors, 2013: Storing and manipulating environmental big data with JASMIN. *IEEE Conf. on Big Data*, Santa Clara, CA, IEEE, 68–75, doi:10.1109/BigData.2013.6691556.

Lindzen, R. S., and S. Nigam, 1987: On the role of sea surface temperature gradients on forcing low-level winds and convergence in the tropics. *J. Atmos. Sci.*, **44**, 2418–2436, doi:10.1175/1520-0469(1987)044<2418:OTROSS>2.0.CO;2.

Ma, J., S. P. Xie, and Y. Kosaka, 2012: Mechanisms for tropical tropospheric circulation change in response to global warming. *J. Climate*, **25**, 2979–2994, doi:10.1175/JCLI-D-11-00048.1.

Maroon, E. A., D. M. W. Frierson, S. M. Kang, and J. Scheff, 2016: The precipitation response to an idealized subtropical continent. *J. Climate*, **29**, 4543–4564, doi:10.1175/JCLI-D-15-0616.1.

Martin, G. M., and Coauthors, 2011: The HadGEM2 family of Met Office Unified Model climate configurations. *Geosci. Model Dev.*, **4**, 723–757, doi:10.5194/gmd-4-723-2011.

Ming, Y., V. Ramaswamy, and G. Persad, 2010: Two opposing effects of absorbing aerosols on global-mean precipitation. *Geophys. Res. Lett.*, **37**, L13701, doi:10.1029/2010GL042895.

Mitchell, J. F. B., C. A. Wilson, and W. M. Cunnington, 1987: On CO_2 climate sensitivity and model dependence of results. *Quart. J. Roy. Meteor. Soc.*, **113**, 293–322, doi:10.1002/qj.49711347517.

Neelin, J. D., and I. M. Held, 1987: Modeling tropical convergence based on the moist static energy budget. *Mon. Wea. Rev.*, **115**, 3–12, doi:10.1175/1520-0493(1987)115<0003:MTCBOT>2.0.CO;2.

Oueslati, B., S. Bony, C. Risi, and J. Dufresne, 2016: Interpreting the inter-model spread in regional precipitation projections in the tropics: Role of surface evaporation and cloud radiative effects. *Climate Dyn.*, **47**, 2801–2815, doi:10.1007/s00382-016-2998-6.

Pierrehumbert, R. T., 1995: Thermostats, radiator fins, and the local runaway greenhouse. *J. Atmos. Sci.*, **52**, 1784–1806, doi:10.1175/1520-0469(1995)052<1784:TRFATL>2.0.CO;2.

Previdi, M., 2010: Radiative feedbacks on global precipitation. *Environ. Res. Lett.*, **5**, 025211, doi:10.1088/1748-9326/5/2/025211.

Rowell, D. P., and R. G. Jones, 2006: Causes and uncertainty of future summer drying over Europe. *Climate Dyn.*, **27**, 281–299, doi:10.1007/s00382-006-0125-9.

Scheff, J., and D. M. W. Frierson, 2012: Robust future precipitation declines in CMIP5 largely reflect the poleward expansion of model subtropical dry zones. *Geophys. Res. Lett.*, **39**, L18704, doi:10.1029/2012GL052910.

Schmidt, G. A., and Coauthors, 2014: Configuration and assessment of the GISS ModelE2 contributions to the CMIP5 archive. *J. Adv. Model. Earth Syst.*, **6**, 141–184, doi:10.1002/2013MS000265.

Schneider, E. K., 1977: Axially symmetric steady-state models of the basic state for instability and climate studies. Part II. Nonlinear calculations. *J. Atmos. Sci.*, **34**, 280–296, doi:10.1175/1520-0469(1977)034<0280:ASSSMO>2.0.CO;2.

Shaw, T. A., 2014: On the role of planetary-scale waves in the abrupt seasonal transition of the Northern Hemisphere general circulation. *J. Atmos. Sci.*, **71**, 1724–1746, doi:10.1175/JAS-D-13-0137.1.

Sobel, A. H., and C. S. Bretherton, 2000: Modeling tropical precipitation in a single column. *J. Climate*, **13**, 4378–4392, doi:10.1175/1520-0442(2000)013<4378:MTPIAS>2.0.CO;2.

Sutton, R. T., B. Dong, and J. M. Gregory, 2007: Land/sea warming ratio in response to climate change: IPCC AR4 model results and comparison with observations. *Geophys. Res. Lett.*, **34**, L02701, doi:10.1029/2006GL028164.

Taylor, K. E., R. J. Stouffer, and G. A. Meehl, 2012: An overview of CMIP5 and the experiment design. *Bull. Amer. Meteor. Soc.*, **93**, 485–498, doi:10.1175/BAMS-D-11-00094.1.

Vecchi, G. A., and B. J. Soden, 2007: Global warming and the weakening of the tropical circulation. *J. Climate*, **20**, 4316–4340, doi:10.1175/JCLI4258.1.

Voldoire, A., and Coauthors, 2013: The CNRM-CM5.1 global climate model: Description and basic evaluation. *Climate Dyn.*, **40**, 2091–2121, doi:10.1007/s00382-011-1259-y.

Volodin, E. M., N. A. Dianskii, and A. V. Gusev, 2010: Simulating present-day climate with the INMCM4.0 coupled model of the atmospheric and oceanic general circulations. *Izv. Atmos. Ocean. Phys.*, **46**, 414–431, doi:10.1134/S000143381004002X.

von Salzen, K., and Coauthors, 2013: The Canadian Fourth Generation Atmospheric Global Climate Model (CanAM4). Part I: Representation of physical processes. *Atmos.–Ocean*, **51**, 104–125, doi:10.1080/07055900.2012.755610.

Watanabe, M., and Coauthors, 2010: Improved climate simulation by MIROC5: Mean states, variability, and climate sensitivity. *J. Climate*, **23**, 6312–6335, doi:10.1175/2010JCLI3679.1.

Watanabe, S., and Coauthors, 2011: MIROC-ESM: Model description and basic results of CMIP5-20c3m experiments. *Geosci. Model Dev.*, **4**, 845–872, doi:10.5194/gmdd-4-1063-2011.

Webb, M. J., and Coauthors, 2015: The impact of parametrized convection on cloud feedback. *Philos. Trans. Roy. Soc. London*, **373A**, 20140414, doi:10.1098/rsta.2014.0414.

Wills, R. C., M. P. Byrne, and T. Schneider, 2016: Thermodynamic and dynamic controls on changes in the zonally anomalous hydrological cycle. *Geophys. Res. Lett.*, **43**, 4640–4649, doi:10.1002/2016GL068418.

Wu, T., and Coauthors, 2014: An overview of BCC climate system model development and application for climate change studies. *Acta Meteor. Sin.*, **28**, 34–56, doi:10.1007/s13351-014-3041-7.

Wyant, M. C., C. S. Bretherton, and P. N. Blossey, 2009: Subtropical low cloud response to a warmer climate in a superparameterized climate model. Part I: Regime sorting and physical mechanisms. *J. Adv. Model. Earth Syst.*, **1** (7), doi:10.3894/JAMES.2009.1.7.

Xie, S., C. Deser, G. A. Vecchi, J. Ma, H. Teng, and A. T. Wittenberg, 2010: Global warming pattern formation: Sea surface temperature and rainfall. *J. Climate*, **23**, 966–986, doi:10.1175/2009JCLI3329.1.

Yoshimori, M., and A. J. Broccoli, 2008: Equilibrium response of an atmosphere–mixed layer ocean model to different radiative forcing agents: Global and zonal mean response. *J. Climate*, **21**, 4399–4423, doi:10.1175/2008JCLI2172.1.

Yukimoto, S., and Coauthors, 2012: A new global climate model of the Meteorological Research Institute: MRI-CGCM3—Model description and basic performance. *J. Meteor. Soc. Japan*, **90A**, 23–64, doi:10.2151/jmsj.2012-A02.

Zeng, N., and J. D. Neelin, 1999: A land–atmosphere interaction theory for the tropical deforestation problem. *J. Climate*, **12**, 857–872, doi:10.1175/1520-0442(1999)012<0857:ALAITF>2.0.CO;2.

Zhang, L., and T. Li, 2016a: Relative roles of anthropogenic aerosols and greenhouse gases in land and oceanic monsoon changes during past 156 years in CMIP5 models. *Geophys. Res. Lett.*, **43**, 5295–5301, doi:10.1002/2016GL069282.

——, and ——, 2016b: Relative roles of differential SST warming, uniform SST warming and land surface warming in determining the Walker circulation changes under global warming. *Climate Dyn.*, **48**, 987–997, doi:10.1007/s00382-016-3123-6.